Korean J Physiol Pharmacol 2023;27(2):131-141
https://doi.org/10.4196/kjpp.2023.27.2.131

KJPP

Original Article

Hsa_circ_0129047 sponges miR-665 to attenuate lung adenocarcinoma progression by upregulating protein tyrosine phosphatase receptor type B

Xiaofan Xia#, Jinxiu Fan#, and Zhongjie Fan*

Department of Respiratory and Critical Care Medicine, Wuhan Red Cross Hospital, Wuhan No.11 Hospital, Wuhan 430015, China

ARTICLE INFO

Received May 10, 2022
Revised December 26, 2022
Accepted January 2, 2023

***Correspondence**
Zhongjie Fan
E-mail: zhongjiefan9@163.com

Key Words
Adenocarcinoma
circ_0129047
Lung
miR-665
PTPRB

#These authors contributed equally to this work.

ABSTRACT Compelling evidence has demonstrated the critical role of circular RNAs (circRNAs) during lung adenocarcinoma (LUAD) progression. Herein, we explored a novel circRNA, circ_0129047, and detailed its mechanism of action. The expression of circ 0129047, microRNA-665 (miR-665), and protein tyrosine phosphatase receptor type B (PTPRB) in LUAD tissues and cells was determined using reverse transcription quantitative polymerase chain reaction and Western blotting. Cell Counting Kit-8 and colony formation assays were conducted to detect LUAD cell proliferation, and western blotting was performed to quantify apoptosis-related proteins (Bcl-2 and Bax). Luciferase reporter and RNA immunoprecipitation assays were used to validate the predicted interaction between miR-665 and circ_0129047 or PTPRB. A xenograft assay was used for the *in vivo* experiments. Circ_0129047 and PTPRB were downregulated in LUAD tissues and cells, whereas miR-665 expression was upregulated. Overexpression of circ_0129047 suppresses LUAD growth *in vivo* and *in vitro*. Circ_0129047 is the target of miR-665, and the miR-665 mimic ablated the anti-proliferative and pro-apoptotic phenotypes of LUAD cells by circ_0129047 augmentation. MiR-665 targets the 3′UTR of PTPRB and downregulates PTPRB expression. PTPRB overexpression offsets the pro-proliferative potential of miR-665 in LUAD cells. Circ_0129047 sequestered miR-665 and upregulated PTPRB expression, thereby reducing LUAD progression, suggesting a promising approach for preventing LUAD.

INTRODUCTION

Due to the high metastasis and recurrence rates, lung adenocarcinoma (LUAD) is the leading cause of lung cancer (LC)-associated deaths despite comprising only 40% of the LC cases in 2020 [1]. Despite the immense efforts in LUAD detection and therapy, the overall survival of patients with LUAD is still less than five years [2]. Thus, understanding the key factors associated with LUAD malignancy might offer novel insights for exploring promising fingerprints for LUAD diagnosis and intervention.

Circular RNAs (circRNAs), a subfamily of non-coding RNAs, are distinguished by their covalently closed loop structures and resistance to RNA exonucleases [3]. The dysregulation of circRNAs plays a significant role during the onset and progression of various cancers, including LUAD [4]. For instance, circRNA-002178 upregulates the expression of programmed death-ligand 1, leading to tumor immune escape and permits LUAD development [5]. CircRNA-ENO1 enhances the expression of enolase 1 (ENO1), increasing the risk of LUAD progression [6]. Furthermore, circRNA_102231 is highly expressed in LUAD tissues and closely associated with advanced clinical outcomes [7]. However, the role of other circRNAs in LUAD remains unclear.

Reportedly, the competitive endogenous RNA (ceRNA) mechanism is favored by circRNAs in tumors [4]. The circRNAs recog-

Author contributions: The tests and data analysis were carried out by X.X. and J.F. The research was created and designed by X.X. Z.F. acquired the data. X.X. and J.F. conducted the interpretation of data. All authors have read and approved this manuscript.

nize miRNAs *via* miRNA response elements and abrogate miRNA silencing on mRNA expression. For example, the circRNA CircZMYM4 works as a ceRNA for miR-587 to delay LUAD metastasis [8]. CircFBXW7 targets miR-942-5p and arrests LUAD cell proliferation, migration, and invasion [9]. Therefore, we need to understand the mechanism of circRNA as ceRNA activity to uncover the underlying mechanism of LUAD progression.

miRNAs are about 22 nucleotides long small non-coding transcripts. They can silence gene expression by undergoing complementary base pairing at the 3′UTR of a target mRNA [10]. miR-655 plays different roles in tumors. For example, miRNA-665 serves as a tumor suppressor in gastric [11] and ovarian cancer [12], whereas it has an oncogenic role in breast [13] and bladder cancer [14]. However, a discrepant role of miR-665 has been described in ovarian cancer [15,16]. Therefore, the function of miR-665 in tumors is cell-context-dependent. Moreover, miR-665 is a regulator in LUAD [17,18]. Therefore, it is important to investigate the regulatory mechanisms between circ_0129047 and miR-665.

The protein tyrosine phosphatase receptor type B (*PTPRB*) gene is present at 12q15 and comprises 37 exons. It encodes a member of the protein tyrosine phosphatase (PTP) family—a signaling molecule that regulates a variety of cellular processes, including cell growth, differentiation, mitotic cycle, and oncogenic transformation [19]. Qi *et al*. [20] showed that *PTPRB* was downregulated in patients with non-small cell lung cancer (NSCLC) and was related to patient prognosis. Its overexpression reduced proliferation and invasion. However, the effect of miR-665 on *PTPRB* expression in LUAD remains unclear.

In the present study, we identified a novel circRNA, circ_0129047 that was downregulated in the LUAD cells and tissues. Furthermore, we found an evident cytoplasmic abundance of circ_0129047 in LUAD cells. Therefore, apart from the biofunction of circ_0129047 in LUAD, circ_0129047-miR-665-PTPRB axis is also of interest. This study may provide a theoretical basis for circRNA application in LUAD diagnosis and therapy.

METHODS

Tissue sample collection

From March 2020 to January 2021, 45 paired tumor tissues and corresponding uncancerous tissues were obtained from LUAD patients at the Wuhan Red Cross Hospital. Written informed consent was obtained from all the patients. None of the patients had undergone preoperative radiochemotherapy. Tissues were subjected to pathological verification after surgery. This study was approved by the Institutional Ethics Committee of the Wuhan Red Cross Hospital (approval number: 2020027).

Cell cultivation

Human bronchial epithelium (BEAS-2B, cat#: CRL-9609), LUAD cells (A549, cat#: CRM-CCL-185 derived from the lung tissue of a white, 58-year-old male with LUAD; H1975, CRL-5908 derived from the lung tissue of a nonsmoking female with LUAD; and Calu-3, cat#: HTB-55, derived from the lung tissue of a white, 25-year-old male with LUAD) were obtained from the American Type Culture Collection (ATCC), and PC9 (cat#: 90071810, derived from the lung tissue of an undifferentiated patient with LUAD) was obtained from Sigma-Aldrich. Calu-3 (Eagle's Minimum Essential medium, Thermo Fisher Scientific), PC9 and H1975 (RPMI-1640 Medium, Thermo Fisher Scientific), A549 (F-12K Medium, Thermo Fisher Scientific), and BEAS-2B (BEBM medium, Thermo Fisher Scientific) were cultivated at 37°C with 5% CO_2 in medium containing 10% fetal bovine serum (Thermo Fisher Scientific) and 1% penicillin/streptomycin (Thermo Fisher Scientific).

Cell transfection

Lentivirus-overexpressing circ_0129047 particles (OE-circ) and their negative control (OE-NC), miR-665 mimic or mimic-NC, empty plasmid (OE-NC), and pcDNA-PTPRB plasmid (OE-PTPRB) were obtained from HanBio Technology Co. Ltd. For transfection of miR-665 mimic or mimic-NC and pcDNA-PTPRB plasmid and their empty plasmid, they were introduced into 80% confluent PC9 and Calu-3 cells using the DharmaFECT1 Transfection Reagent (Horizon) according to the manufacturer's protocol. For lentivirus transfection, virus particles produced at 10 multiplicity of infection were delivered into PC9 and Calu-3 cells. After 48 h, the cells were transferred in puromycin-containing media. The puromycin-resistant colonies were propagated after a two-week selection. Transfection efficiency was determined using reverse transcription quantitative polymerase chain reaction (RT-qPCR).

RT-qPCR assay

A MolPure Cell RNA Kit (Yeasen) was used to obtain total RNA from the LUAD tissues and cells. RNAs was reverse-transcribed into cDNA using the miRNA 1st Strand cDNA Synthesis Kit (Vazyme) or PrimeScript RT reagent Kit (Takara). The resultant cDNA was amplified and quantified using real-time PCR using a real-time PCR fluorescence quantitative kit (Solarbio) on a 7900HT real-time PCR system. The outcome was normalized to the internal interference (U6 and GDPAH) using the $2^{-\Delta\Delta Ct}$ method [21]. The primers used are listed in Table 1.

Cell nuclear/cytoplasmic fraction isolation

We used a cytoplasmic and nuclear RNA purification kit ob-

Table 1. Real-time PCR primer synthesis list

Gene		Sequences
miR-665	Forward	5'-TCTCCTCGAGGGGTCTCTG-3'
	Reverse	5'-CCGCCTGTGAGGGGC-3'
PTPRB	Forward	5'-CCCAAGCGAAGCATGAACAG-3'
	Reverse	5'-TCACCGAAACTTCTGCTCCC-3'
U6	Forward	5'-CTCGCTTCGGCAGCACA-3'
	Reverse	5'-AACGCTTCACGAATTTGCGT-3'
GAPDH	Forward	5'-AGAAAAACCTGCCAAATATGATGAC-3'
	Reverse	5'-TGGGTGTCGCTGTTGAAGTC-3'

tained from Norgen Biotek Corp. USA to prepare the nuclear and cytoplasmic parts of PC9 and Calu-3 cells according to the manufacturer's instructions. Circ_0129047 in the nuclear and cytoplasmic parts of the cells was quantified using RT-qPCR.

RNase treatment

Total RNA (2 μg) from PC9 and Calu-3 cells was digested with or without RNase for 30 min at 37°C. RT-qPCR was performed to determine the expression of circ_0129047 in PC9 and Calu-3 cells exposed to RNase.

Western blot

Cells were homogenized in radioimmunoprecipitation assay (RIPA) lysis buffer. After centrifugation, the supernatant was quantified with the bicinchoninic acid colorimetric (BCA) method. Next, 30 μg of protein was separated on a 10% SDS-PAGE gel and transferred to PVDF membranes in a pre-assembled transfer sandwich process. After blocking with 5% non-fat blocking grade milk at room temperature for 1 h, the membranes were blotted overnight at 4°C with antibodies against Bax (cat#: PA5-39778, 1:1,000, Thermo Fisher Scientific), Bcl-2 (cat#: 13-8800, 1:1,000, Thermo Fisher Scientific), PTPRB (cat#: PA5-119373, 1:1,000, Thermo Fisher Scientific). Anti-rabbit secondary antibody (cat#: sc-3836, 1:5,000, Santa Cruz Biotechnology) and anti-mouse secondary antibodies (cat#: W4021, 1:10,000; Promega) were used to identify the target proteins on the membranes 24 h later. ECL Plus reagents were used to detect the immunoreactive bands (Amersham).

Cell Counting Kit-8 (CCK-8) assay

PC9 and Calu-3 cells (4×10^4 cells/well) were seeded in 96-well plates. After 24, 48, and 72 h of cultivation, the cells were exposed to 10 μl of CCK-8 reagent (Thermo Fisher Scientific). After 3 h, the optical density (OD) at 450 nm was measured for each well using a microplate reader (BioTek).

Colony formation assay

PC9 and Calu-3 cells were plated in 6-well plates at a density of 500 cells/well. After two weeks of cultivation, the colonies were counted and photographed using a microscope (Olympus) after undergoing fixation with 100% methanol (20 min) and staining with 25% crystal violet (30 min). Colonies containing > 50 cells were counted.

In vivo assay

The Wuhan University Center for Animal Experiment/Animal Biosafety Level III laboratory (ABSL-III lab) provided ten female BALB/C nude mice (4–5 weeks old, 20–25 g). The mice were raised under standard culture conditions for a week for acclimatization. For Xenograft tumorigenicity assays, PC9 cells (4×10^4 cells) infected with lentiviral particles harboring circ_0129047-overexpressing vectors or empty vectors were administered subcutaneously into the lateral tail veins of female BALB/C nude mice. Tumor size was monitored every four days. The mice were euthanized by CO_2 inhalation for 28 days, and the final tumor weight was recorded. Tumor volume (mm^3) = length (mm) × $width^2$ (mm^2) / 2. Our hospital's Institutional Animal Care and Ethics Committee approved this experiment (approval number: 20210814).

Luciferase reporter assay

To create circ_0129047-wild type (WT) and PTPRB 3′UTR-WT plasmids, the sequences of circ_0129047 and PTPRB 3′UTR binding to miR-665 were ligated into the pmirGLO dual-luciferase miRNA Target Expression Vector to produce WT luciferase reporter vectors. The corresponding mutant (MUT) vectors of circ_0129047 and PTPRB 3′UTR without the binding sites for miR-665 were established using site-directed mutagenesis using the QuikChange Site-Directed Mutagenesis Kit (Invitrogen). The developed WT and MUT luciferase vectors were co-transfected with the miR-665 mimic or NC mimics into PC9 and Calu-3 cells. After 48 h, luciferase density was determined using the Luciferase Reporter System (Promega).

RNA immunoprecipitation (RIP) assay

The RNA-protein pulldown kit (Thermo Fisher Scientific) was used to detect the association between circ_0129047 and miR-665. Briefly, cell lysates were prepared using Thermo Scientific Pierce IP Lysis Buffer and then incubated with magnetic beads conjugated with Argonaute 2 antibody or IgG antibody. Finally, the pulled RNA-Binding Protein Complexes were washed and eluted. RT-qPCR was conducted to determine circ_012904 and miR-665 expression levels.

Statistical analysis

GraphPad Prism 9.0 was utilized (GraphPad Software Inc.) for statistical analyses. Student's t-test was used to determine statistical significance between two groups, and one-way ANOVA with Tukey's post-test was used to determine statistical significance between two groups. The relationship between miR-665 expression and circ_0129047 or PTPRB expression was investigated using Pearson analysis. $p < 0.05$ was considered statistically significant.

RESULTS

Human circular RNA-0129047 (has_circ_0129047) expression was downregulated in LUAD

First, to evaluate the expression of circ_0129047 in LUAD, we measured circ_0129047 levels in LUAD clinical samples and cells. Simultaneous downregulation of circ_0129047 was detected in LUAD tissues (Fig. 1A) compared with that in the normal tissues. Similarly, circ_0129047 expression was also downregulated in LUAD cells (A549, H1975, PC9, and Calu-3) compared with human bronchial epithelium cells BEAS-2B (Fig. 1B). PC9 and Calu-3 cells presented greater downregulation of circ_0129047. Hence, we chose them for subsequent assays. The annular structure of circ_0129047 is shown in Fig. 1C. RT-qPCR analysis was performed to examine the subcellular localization of circ_0129047 and to fully understand its function. The results showed the predominance of cytoplasmic circ_0129047 in PC9 and Calu-3 cells (Fig. 1D). LIF receptor subunit alpha (LIFR) is a linear transcript of circ-0129047. circRNA is resistant to digestion by the 3′–5′ exoribonuclease, RNase R, while linear mRNA is sensitive to RNase R. Therefore, we performed an RNase R treatment assay to identify the circular feature of circ_0129047. The results showed that LIFR was downregulated after RNase R treatment, but RNase R did not affect circ_0129047, further validating the circular feature of circ_0129047 in PC9 and Calu-3 cells (Fig. 1E). These data suggested that circ_0129047 is downregulated and may be involved in LUAD malignancy.

Augmentation of circ_0129047 expression acts as a tumor suppressor in LUAD *in vitro* and *in vivo*

To ascertain whether circ_0129047 plays a role in LUAD malignancy, we manipulated circ_0129047 expression in PC9 and Calu-3 cells by introducing circ_012904-overexpressing vectors.

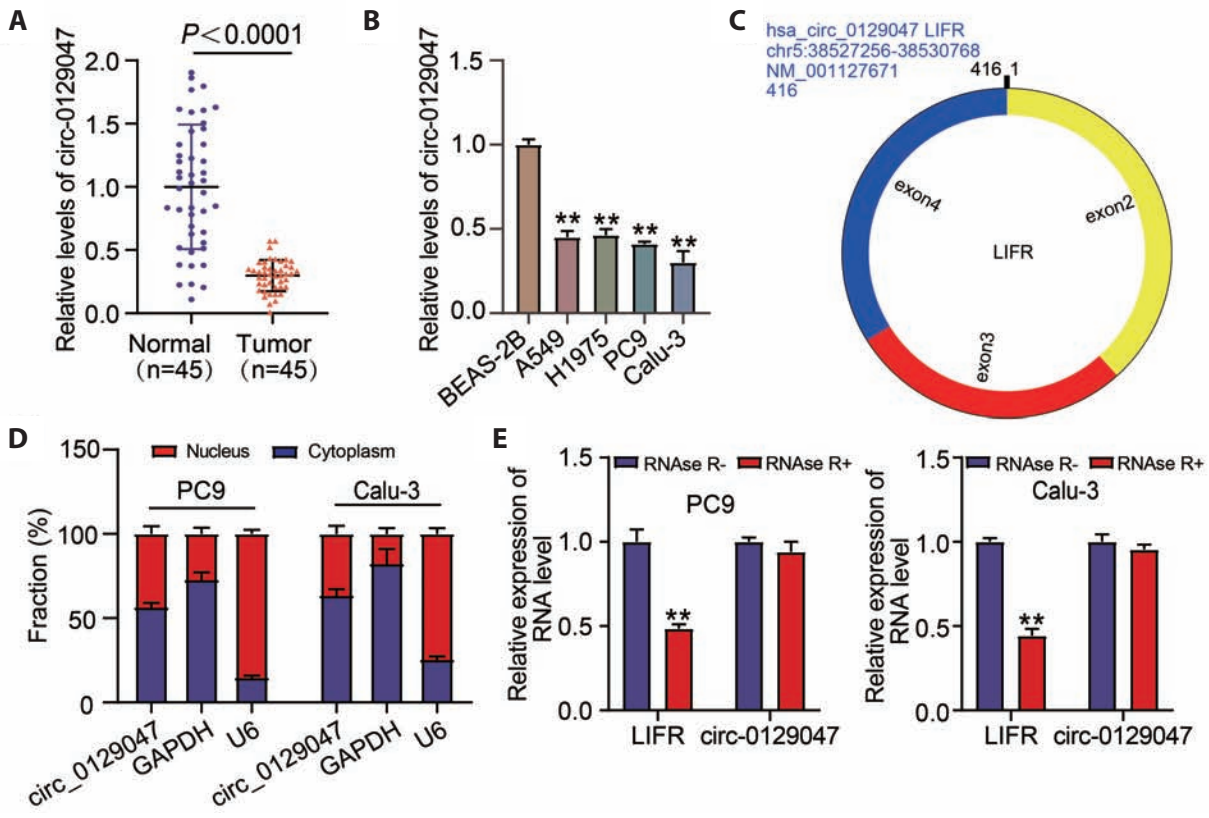

Fig. 1. Hsa_circ_0129047 expression was downregulated in lung adenocarcinoma (LUAD). (A) RT-qPCR analysis results of circ_0129047 in both LUAD and normal tissues. (B) RT-qPCR analysis of circ_0129047 in human bronchial epithelium (BEAS-2B) and LUAD cells (A549, H1975, PC9 and Calu-3). **p < 0.01 *vs*. BEAS-2B. (C) Loop structures of Circ_012904. (D) Subcellular localization of circ_0129047 in PC9 and Calu-3 cells. (E) Circ_012904 was resistant to RNase R digestion. **p < 0.01 *vs*. RNAse R. Values are presented as mean ± SD.

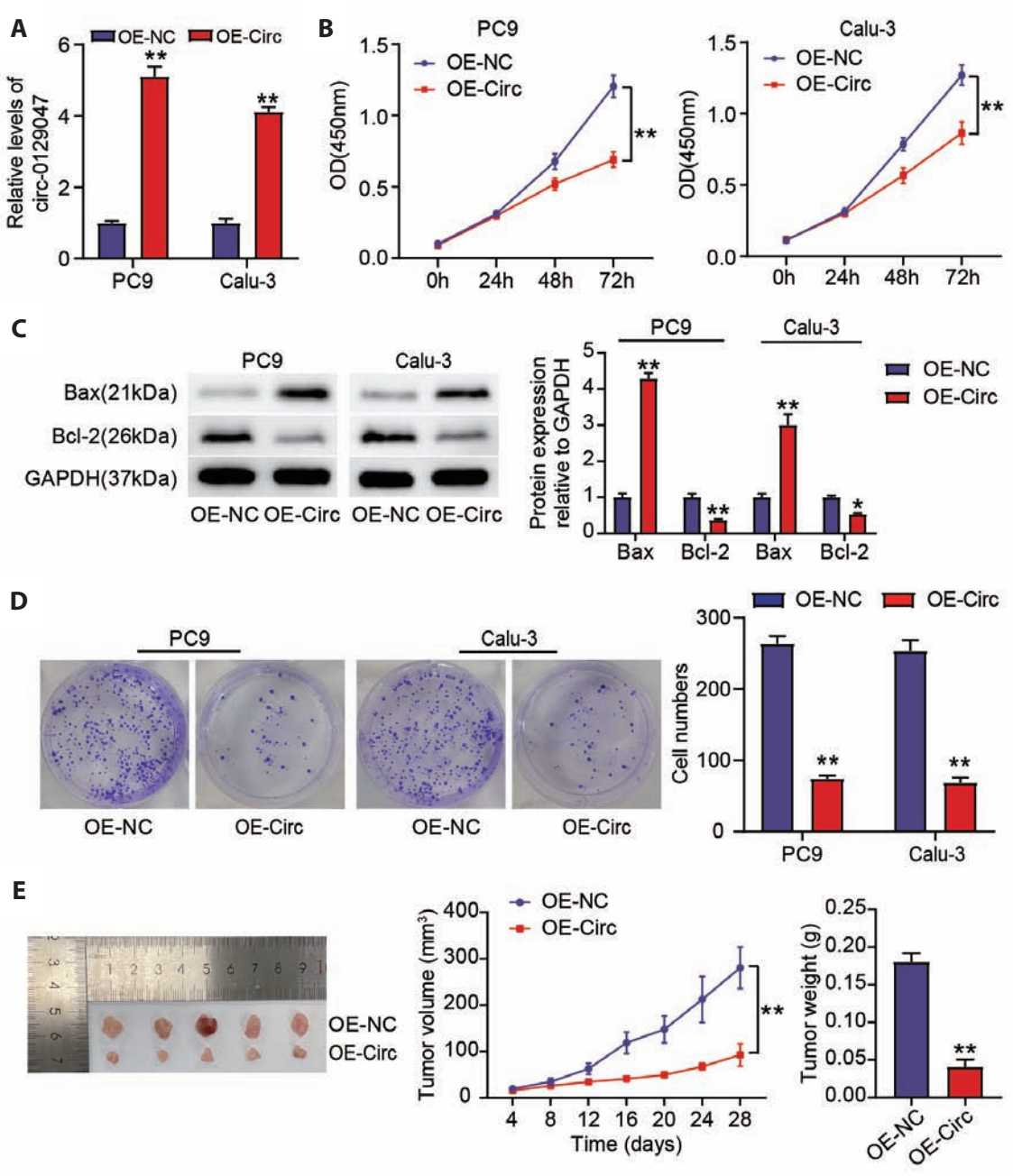

Fig. 2. Augmentation of circ_0129047 expression suppresses LUAD tumors *in vitro* and *in vivo*. circ 0129047-overexpressing vectors (OE-circ) and empty vectors were transfected into PC9 and Calu-3 cells (OE-NC). (A) RT-qPCR analysis of circ_0129047 expression 48 h later. (B) Cell proliferation assay using the CCK-8 assay. (C) Expression of apoptosis-related proteins (Bcl-2 and Bax) determined using Western blotting. (D) Colony formation was assessed using colony formation assay (×200). (E) Xenograft tumor growth assay. Values are presented as mean ± SD. LUAD, lung adenocarcinoma; OD, optical density. **p < 0.01 *vs*. OE-NC.

As shown in Fig. 2A, circ_012904 expression significantly increased. Next, the effects of circ_0129047 overexpression on the proliferation, apoptosis, and tumor growth of LUAD cells were detected using *in vitro* and *in vivo* functional analyses. In the functional analysis, the OD value was reduced after LUAD cells were transfected with circ_0129047 overexpression vectors, suggesting that LUAD cell proliferation was significantly diminished upon circ_0129047 overexpression (Fig. 2B). Furthermore, we found that circ_0129047 overexpression led to the upregulation of Bax and downregulation of Bcl-2, indicative of apoptosis activation (Fig. 2C). Circ_0129047 overexpression reduced the number of cell colonies formed (Fig. 2D). To clarify whether circ_0129047 has a similar importance in LUAD tumorigenesis *in vivo*, we developed a PC9 xenograft mouse model. Within four weeks, tumor weight and size were significantly decreased in the circ_0129047-overexpressing group (Fig. 2E). Simultaneously, circ_0129047

expression was significantly upregulated in the circ_0129047-overexpressing group (Supplementary Fig. 1A). These data suggest that downregulation of circ_0129047 promotes LUAD tumorigenesis, both *in vitro* and *in vivo*.

Circ_0129047 targets miR-665

Given the cytoplasmic enrichment of circ_0129047, we further explored which miRNAs were sponged by circ_0129047 during LUAD progression. Through an online tool circInteractome analysis, we found that miR-665 shared a complementary seed sequence with circ_0129047 (Fig. 3A). To confirm the interaction between circ_0129047 and miR-665, RIP and luciferase reporter assays were performed. In the RIP assay, circ_0129047 and miR-665 were predominantly enriched in the AGO-2 groups (Fig. 3B). In the luciferase reporter assay, the miR-665 mimic induced a decrease in luciferase activity in the circ_0129047 WT group, but luciferase activity in the circ_0129047 MUT group remained unaffected (Fig. 3C). Therefore, circ_0129047 may sponge miR-665 to exert its effects. Interestingly, we also found that miR-665 was amplified in LUAD tissues (Fig. 3D) and LUAD cells (Fig. 3E) compared with the normal tissues and BEAS-2B cells. Moreover, the correlation between circ_0129047 and miR-665 was measured, and their negative correlation with Pearson analysis further supported their targeting action (Fig. 3F). In addition, circ_0129047 inhibited the expression of miR-665 in the tumor

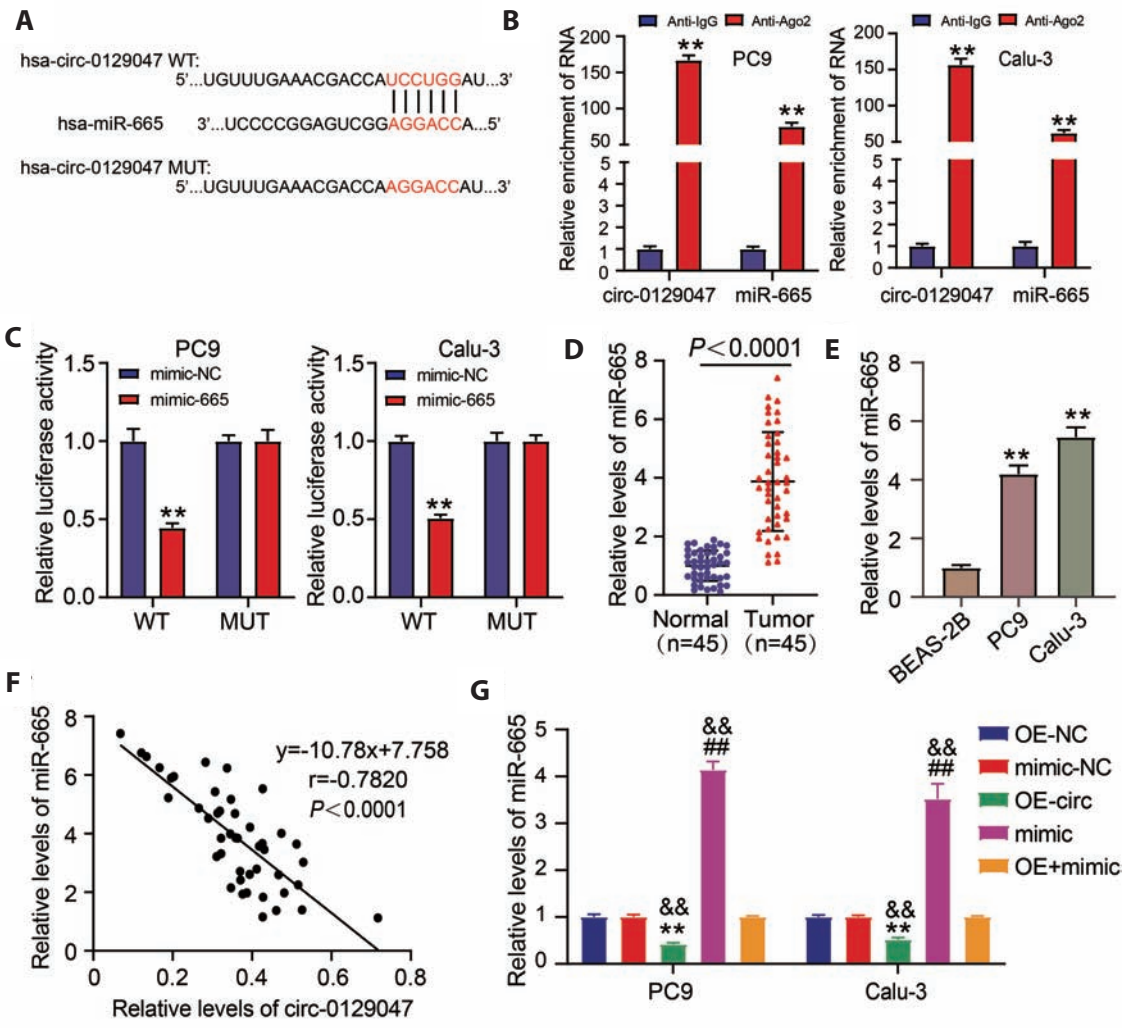

Fig. 3. Circ_0129047 targets miR-665. (A) MiR-665 is predicted as a target of circ_0129047 through CircInteractome. (B) RIP assay was performed using Ago2 antibody in LUAD cells, and the enrichment of circ_0129047 and miR-665 was detected. **p < 0.01 *vs*. Anti-IgG. (C) Luciferase activity of Circ_0129047 in LUAD cells transfected with miR-665 mimics, which bind to the circ 0129047 sequence. **p < 0.01 *vs*. mimic-NC. (D) RT-qPCR analysis of miR-665 in LUAD tissues and normal tissues. (E) RT-qPCR analysis of miR-665 in LUAD cells (PC9 and Calu-3) and normal cells (BEAS-2B). **p < 0.01 *vs*. BEAS-2B. (F) Pearson analysis of miR-665 expression and circ_0129047 expression in LUAD tissues. (G) circ 0129047-overexpressing vectors (OE-circ), OE-NC, miR-665 mimic (mimic), mimic-NC, and OE+mimic were transfected into PC9 and Calu-3 cells. The expression of miR-665 was measured using RT-qPCR 48 h after transfection. **p < 0.01 *vs*. OE-NC; $^{\#\#}$p < 0.01 *vs*. mimic-NC; $^{\&\&}$p < 0.01 *vs*. OE+mimic. Values are presented as mean ± SD. LUAD, lung adenocarcinoma; Ago2, Argonaute 2; WT, wild type; MUT, mutant.

tissues of nude mice (Supplementary Fig. 1B). Transfection of miR-665 mimic and circ_0129047-overexpressing vectors into PC9 and Calu-3 cells showed that miR-665 expression was enhanced by miR-665 mimic and impaired by circ_0129047-overexpressing vectors. However, the effect of the miR-665 mimic on miR-665 expression was recovered by co-transfection with circ_0129047-overexpressing vectors (Fig. 3G). In summary, circ_0129047 sponges miR-665 and downregulates miR-665 expression.

MiR-665 is a critical target *via* which circ_0129047 mediates LUAD tumorigenesis

Based on the target analysis, we clarified the *in vitro* association between miR-665 and circ_0129047 using a series of cell functional experiments. After performing the CCK-8 assay, we found that the miR-665 mimic functioned as a proliferation promoter in PC9 and Calu-3 cells. However, its increased proliferation was mitigated by circ_0129047-augmented expression (Fig. 4A). Apoptosis was inactivated in PC9 and Calu-3 cells treated with the miR-665 mimic, as demonstrated by the reduced expression of Bax and increased expression of Bcl-2. However, this inactivation of apoptosis in LUAD cells was re-elicited by the co-

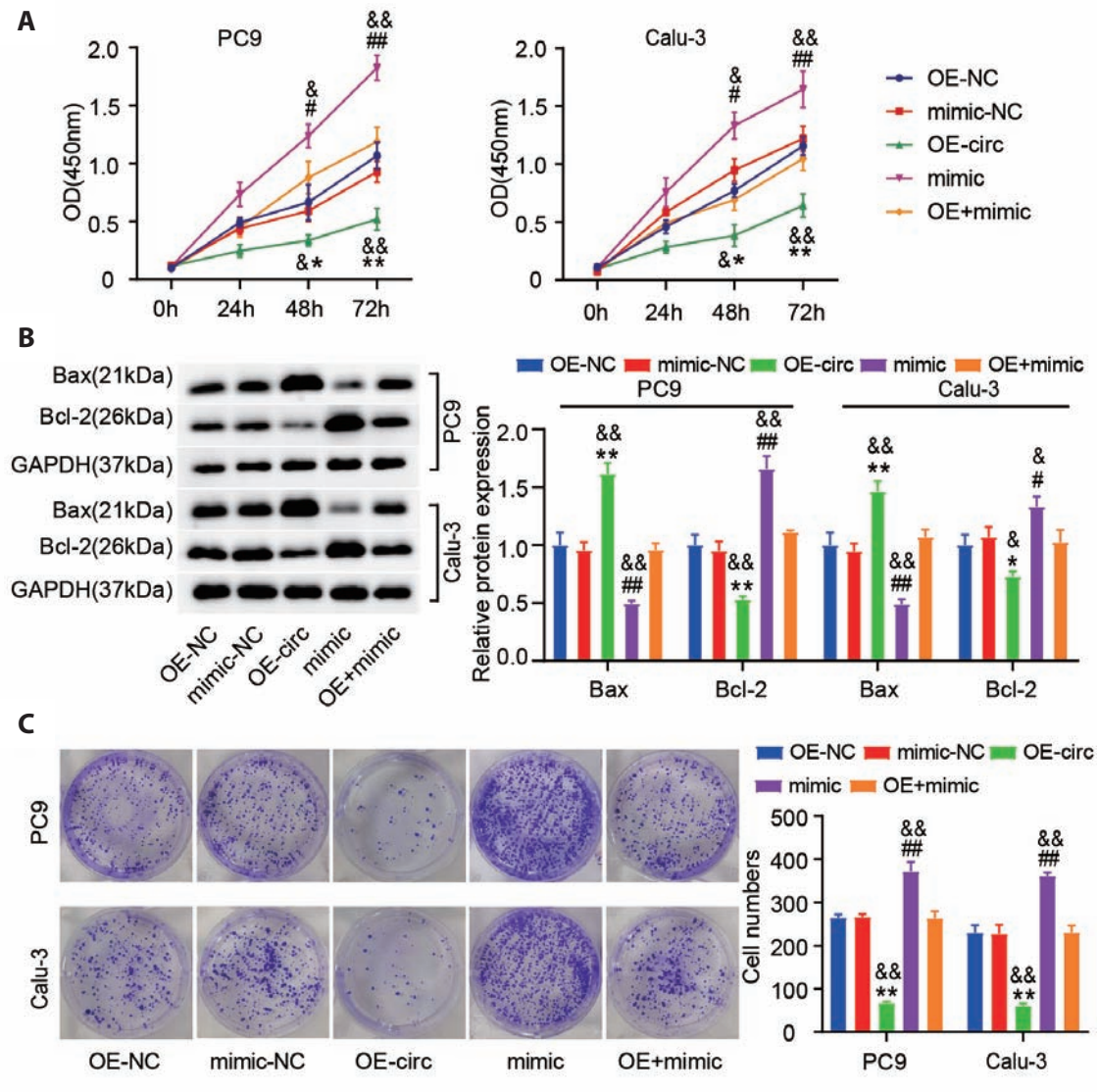

Fig. 4. MiR-665 is a critical target *via* which circ_0129047 mediated LUAD tumorigenesis. PC9 and Calu-3 cells were transfected with circ_0129047 overexpression vectors (OE-circ), OE-NC, miR-665 mimic (mimic) or mimic-NC, and OE+mimic. (A) Cell proliferation was analyzed using the CCK-8 assay. (B) Western blot analysis of anti-Bax and anti-Bcl-2 expression. (C) Colony formation determined using colony formation assay (×200). Values are presented as mean ± SD. LUAD, lung adenocarcinoma; OD, optical density; PTPRB, protein tyrosine phosphatase receptor type B. *p < 0.05, **p < 0.01 *vs*. OE-NC; #p < 0.05, ##p < 0.01 *vs*. mimic-NC; &p < 0.05, &&p < 0.01 *vs*. OE+mimic.

transfection of circ_0129047-overexpressing vectors (Fig. 4B). Overexpression of miR-665 also resulted in higher colony formation ability compared with that of the control group, and this was reversed along with circ_0129047 overexpression (Fig. 4C). Taken together, circ_0129047 suppresses the pro-tumorigenic function of miR-665 in LUDA cells by sequestering miR-665.

MiR-665 targets PTPRB

It is known that circRNAs inhibit mRNA silencing by miRNA through ceRNA activity. Since miRNAs modify mRNA expression by mRNA 3′UTR, we conducted TargetScan analysis to mine the downstream mRNA of miR-665. As shown in Fig. 5A, the PTPRB 3′UTR contained a consequential pairing of miR-665.

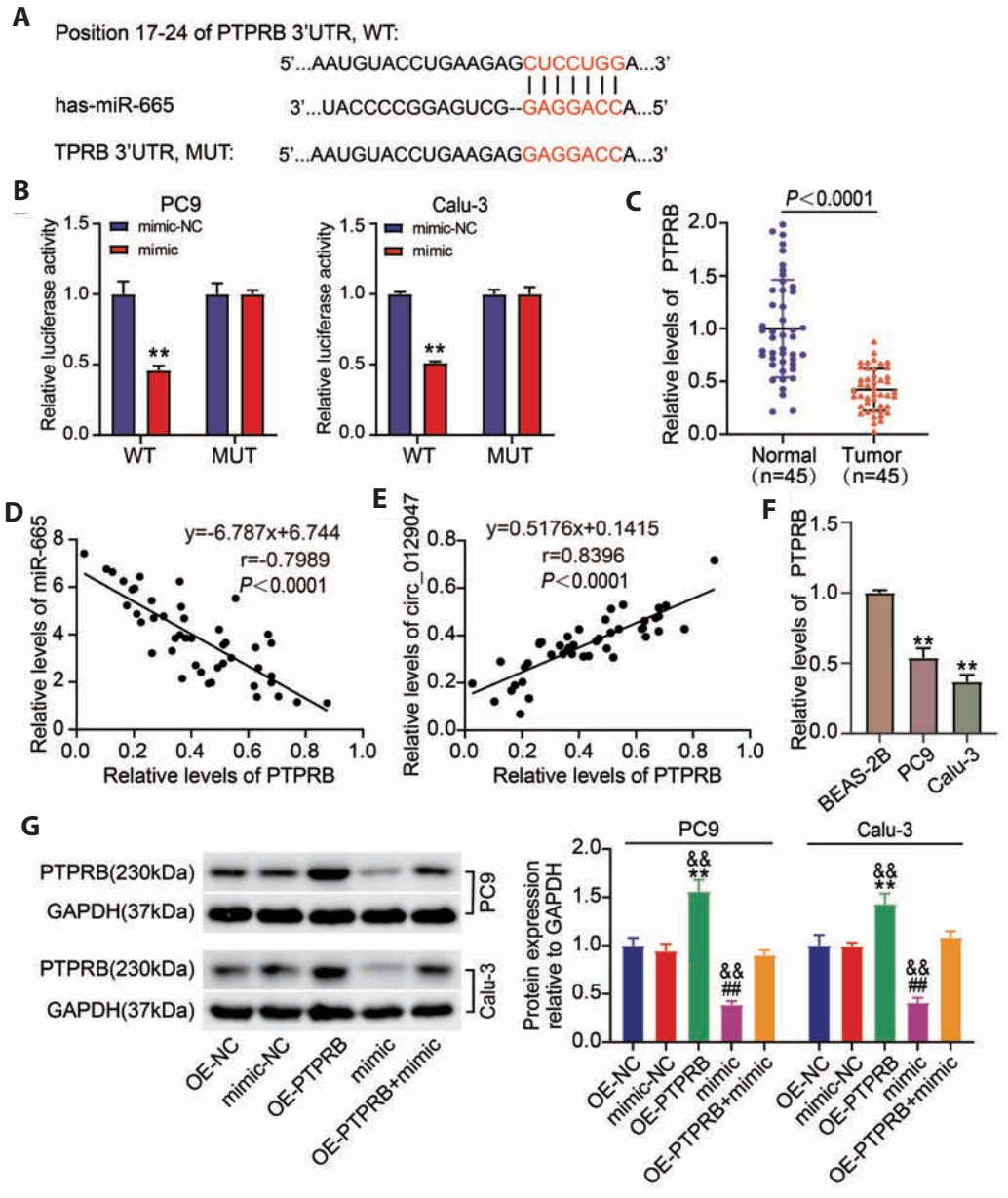

Fig. 5. MiR-665 targets PTPRB. (A) Predicted miR-665 interactions with PTPRB 3′UTR using miRNA target prediction software based on TargetScan. (B) Luciferase reporter gene assay of PTPRB 3′UTR after miR-665 treatment. **p < 0.01 *vs*. mimic-NC. (C) PTPRB mRNA expression in LUAD tissues analyzed using RT-qPCR. (D) Pearson correlation analysis was used to analyze the relationship between miR-665 and PTPRB in LUAD tissues. (E) Pearson correlation analysis was used to analyze the relationship between circ_0129047 and PTPRB in LUAD tissues. (F) PTPRB mRNA expression in LUAD cells (PC9 and Calu-3) and normal cells (BEAS-2B) using RT-qPCR. **p < 0.01 *vs*. BEAS-2B. (G) Western blot analysis determining PTPRB expression in LUAD cells transfected with PTPRB-overexpressing vectors (OE-PTPRB), OE-NC, miR-665 mimic (mimic), mimic-NC, OE-PTPRB+mimic. **p < 0.01 *vs*. OE-NC; $^{\#\#}$p < 0.01 *vs*. mimic-NC; $^{\&\&}$p < 0.01 *vs*. OE-PTPRB+mimic. Values are presented as mean ± SD. LUAD, lung adenocarcinoma; PTPRB, protein tyrosine phosphatase receptor type B; WT, wild type; MUT, mutant.

Next, we cloned the consequential pairing region and MUT sequence into luciferase reporter vectors and detected luciferase activity of the PTPRB 3′UTR in LUAD cells. Undoubtedly, PTPRB 3′UTR-mediated luciferase activity was reduced in miR-665 overexpressing LUAD cells, and once PTPRB 3′UTR was mutated, the luciferase activity was restored (Fig. 5B). We found that PTPRB was poorly expressed in the clinical samples (Fig. 5C). Furthermore, the poor expression of PTPRB was negatively correlated with miR-665 (Fig. 5D), consistent with our putative targeting relationship between the PTPRB 3′UTR and miR-665. In addition, PTPRB levels in LUAD tissues were positively correlated with circ_012947 (Fig. 5E), and the nude mice assay further proved that the overexpression of circ_0129047 enhanced the expression of PTPRB in the tumor tissues of nude mice (Supplementary Fig. 1C). Low PTPRB expression was also observed in LUAD cells compared with that in BEAS-2B cells (Fig. 5F). After transfecting the miR-665 mimic and PTPRB overexpression vectors into PC9 and Calu-3 cells, western blotting showed that PTPRB expression was elevated by the PTPRB overexpression vector and reduced by the miR-665 mimic. However, the PTPRB overexpression vector recovered the loss of PTPRB expression in LUAD cells induced by the miR-665 mimic (Fig. 5G). Hence, miR-665 directly targeted PTPRB and silenced its expression in LUAD cells.

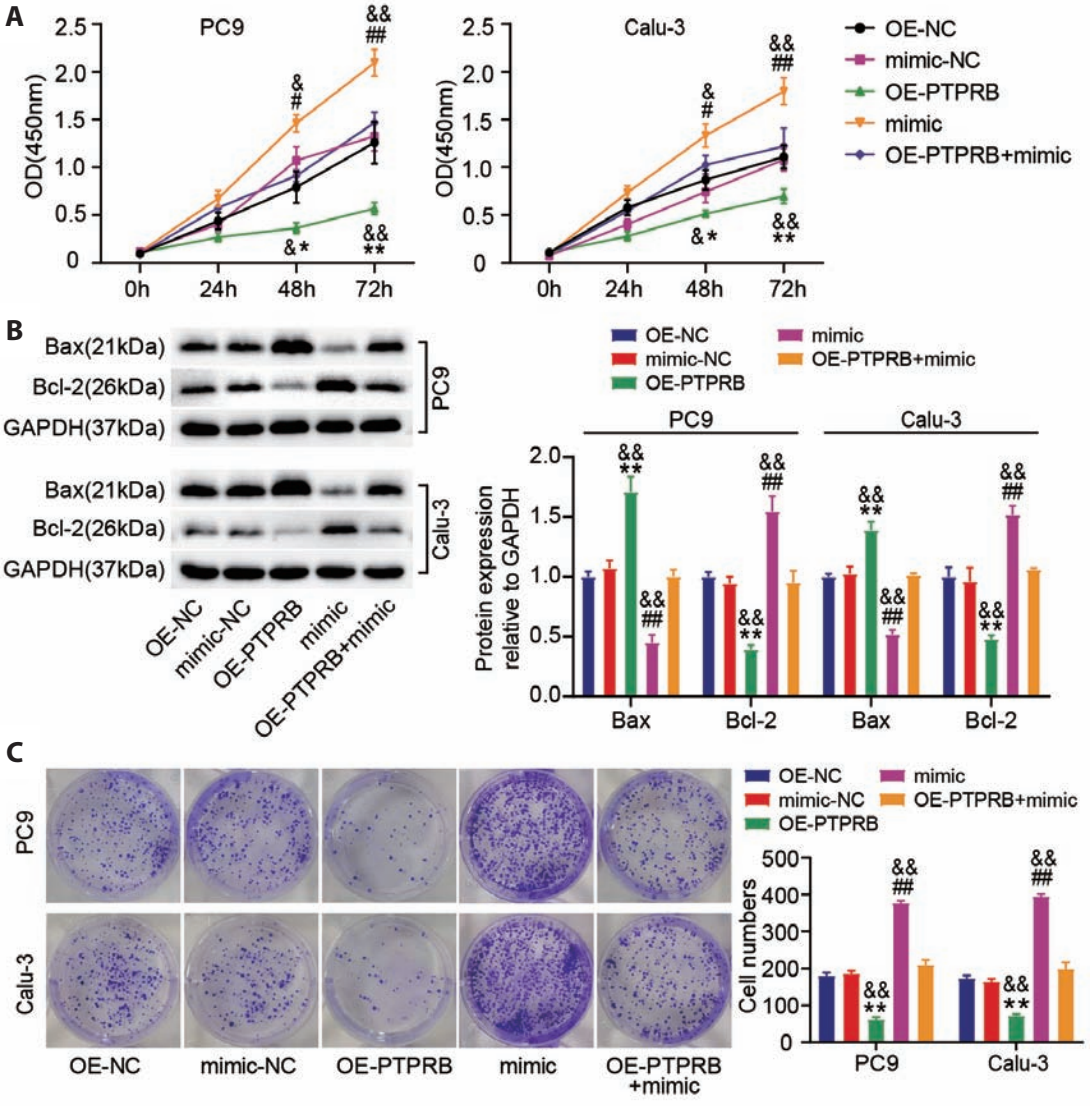

Fig. 6. The tumorigenic role of miR-665 may be achieved by targeting PTPRB 3′UTR. LUAD cells were transfected with PTPRB-overexpressing vectors (OE-PTPRB), OE-NC, miR-665 mimic (mimic), mimic-NC, and OE-PTPRB+mimic. (A) Cell proliferation was analyzed using the CCK-8 assay. (B) Western blot analysis of anti-Bax and anti-Bcl-2 expression in the transfected cells. (C) Colony formation was determined using colony formation assay (×200). *$p < 0.05$, **$p < 0.01$ *vs*. OE-NC; $^{\#}p < 0.05$, $^{\#\#}p < 0.01$ *vs*. mimic-NC; $^{\&}p < 0.05$, $^{\&\&}p < 0.01$ *vs*. OE-PTPRB+mimic. Values are presented as mean ± SD. LUAD, lung adenocarcinoma; OD, optical density; PTPRB, protein tyrosine phosphatase receptor type B.

The tumorigenic role of miR-665 may be achieved by targeting PTPRB 3′UTR

Our findings indicate that miR-665 interferes with PTPRB expression by targeting the 3′UTR of PTPRB. Hence, we subsequently investigated the effects of PTPRB on the pro-tumorigenic potential of miR-665 using cell function experiments. In the CCK-8 assay, PTPRB overexpression inhibited LUAD cell proliferation, but this effect was abrogated by co-transfection with the miR-665 mimic (Fig. 6A). Western blotting showed that PTPRB overexpression enhanced Bax expression and reduced Bcl-2 expression, suggesting that PTPRB overexpression elicited apoptosis. However, the promotive effect of PTPRB overexpression on apoptosis was reversed by the miR-665 mimic (Fig. 6B). The colony formation assay revealed that ectopic expression of PTPRB reduced the number of colonies formed, but miR-665 mimic-mediated enhancement of cell colony formation relieved the inhibitory effect of PTPRB ectopic expression on the colony formation (Fig. 6C). Therefore, miR-665 may favor LUAD malignant behaviors by targeting the PTPRB 3′UTR.

DISCUSSION

Dysregulation of circRNAs is a common cascade involving many cellular and physiological processes, including ontogenesis [22]. Their biological importance has also been depicted in LUAD [23]. However, circRNAs in LUAD remain largely unknown. Herein, we describe an unrecognized circRNA, circ_0129047, which is downregulated in LUAD. Functional investigation revealed that circ_0129047, a tumor suppressor, inhibited LUAD growth *in vitro* and *in vivo*. Further mechanistic exploration revealed a circ_0129047/miR-665/PTPRB ceRNA regulatory network during LUAD in malignant lesions and underscored the potential of circ_0129047 in clinical applications.

Growing evidence has shown that cytoplasmic circRNAs have sponging properties against miRNAs [24]. Intriguingly, we also found subcellular localization of circ_0129047 in the cytoplasm. Therefore, it is reasonable to explore the effects of ceRNA in LUAD. We found that circ_0129047 targets miR-665 through circRNA interactome prediction and validation from luciferase reporter and RIP assays. Interestingly, a paradoxical role for miR-665 has been reported in LUAD. For example, Ying *et al*. [17] demonstrated that miR-665 targeted by circ-TSPAN4 promotes LUAD metastasis. However, miR-665 targeted by circ-000881 suppresses the malignant behaviors [18]. Therefore, the role of miR-665 in LUAD remains unclear. Our data showed that augmented miR-665 expression strengthened the LUAD cell proliferation and inhibited apoptosis, suggesting its pro-tumorigenic role in LUAD. Further mechanical exploration showed that circ_0129047 attenuated the increase in LUAD cell proliferative potential induced by miR-665. Therefore, circ_0129047 may target miR-665 and downregulate the pro-proliferative potential of miR-665, resulting in LUAD suppression.

PTPRB plays different roles in various cancers. PTPRB overexpression enhances the oncogenic phenotypes of cervical cancer *in vitro* [25], whereas it is poorly expressed in hepatocellular carcinoma and could weaken oncogenic Hippo signaling, mitigating tumor growth [26]. In addition, PTPRB was found to be a carcinogenic factor in NSCLC [20]. In the present study, we found that PTPRB was downregulated in LUAD tissues, and its overexpression caused a proliferative defect in LUAD cells accompanied by apoptosis activation. Our findings provide evidence for tumor suppression in NSCLC, as evidenced by the fact that PTPRB overexpression abrogates the malignant action of cancer cells [27,28]. Mechanistically, we found that miR-665 silences PTPRB expression. Our findings provide further evidence for the tumor-suppressive role of PTPRB in LUAD.

Our investigation identified a novel circRNA, circ_0129047, in LUAD. However, our study has some limitations. First, the downstream pathway components of PTPRB that weaken the tumorigenic potential of LUAD remain unknown. PTPRB silencing boosts the Src phosphorylation and favors LC progression [20]. Thus, in the near future, we will uncover the detailed mechanisms underlying LUAD progression. Furthermore, owing to the imperfect base pairing, circRNAs are embedded in complex regulatory ceRNA networks, including different miRNAs or mRNAs. Therefore, it is necessary to elucidate the mechanism underlying circ_0129047-mediated LUAD progression.

Our findings revealed that circ_0129047 mitigated LUAD proliferation *in vitro* and restricted its progression *in vivo*. Furthermore, circ_0129047 acted as a ceRNA for miR-665 to abrogate the inhibition of miR-665 by PTPRB, thereby interfering with LUAD cell proliferation. Our findings might be helpful in uncovering the mechanism of LUAD progression and suggest that targeting circ_012904 might have promising prospects for LUAD intervention.

FUNDING

None to declare.

ACKNOWLEDGEMENTS

None.

CONFLICTS OF INTEREST

The authors declare no conflicts of interest.

SUPPLEMENTARY MATERIALS

Supplementary data including one figure can be found with this article online at https://doi.org/10.4196/kjpp.2023.27.2.131

REFERENCES

1. Sung H, Ferlay J, Siegel RL, Laversanne M, Soerjomataram I, Jemal A, Bray F. Global cancer statistics 2020: GLOBOCAN estimates of incidence and mortality worldwide for 36 cancers in 185 countries. *CA Cancer J Clin.* 2021;71:209-249.
2. Sun GZ, Zhao TW. Lung adenocarcinoma pathology stages related gene identification. *Math Biosci Eng.* 2019;17:737-746.
3. Kristensen LS, Andersen MS, Stagsted LVW, Ebbesen KK, Hansen TB, Kjems J. The biogenesis, biology and characterization of circular RNAs. *Nat Rev Genet.* 2019;20:675-691.
4. Lei M, Zheng G, Ning Q, Zheng J, Dong D. Translation and functional roles of circular RNAs in human cancer. *Mol Cancer.* 2020;19:30.
5. Li J, Zhang F, Li H, Peng F, Wang Z, Peng H, He J, Li Y, He L, Wei L. Circ_0010220-mediated miR-503-5p/CDCA4 axis contributes to osteosarcoma progression tumorigenesis. *Gene.* 2020;763:145068.
6. Zhou J, Zhang S, Chen Z, He Z, Xu Y, Li Z. CircRNA-ENO1 promoted glycolysis and tumor progression in lung adenocarcinoma through upregulating its host gene ENO1. *Cell Death Dis.* 2019;10:885.
7. Zong L, Sun Q, Zhang H, Chen Z, Deng Y, Li D, Zhang L. Increased expression of circRNA_102231 in lung cancer and its clinical significance. *Biomed Pharmacother.* 2018;102:639-644.
8. Yuan DF, Wang HR, Wang ZF, Liang GH, Xing WQ, Qin JJ. CircRNA CircZMYM4 inhibits the growth and metastasis of lung adenocarcinoma via the miR-587/ODAM pathway. *Biochem Biophys Res Commun.* 2021;580:100-106.
9. Dong Y, Qiu T, Xuan Y, Liu A, Sun X, Huang Z, Su W, Du W, Yun T, Wo Y, Navarro A, Jiao W. circFBXW7 attenuates malignant progression in lung adenocarcinoma by sponging miR-942-5p. *Transl Lung Cancer Res.* 2021;10:1457-1473.
10. Correia de Sousa M, Gjorgjieva M, Dolicka D, Sobolewski C, Foti M. Deciphering miRNAs' action through miRNA editing. *Int J Mol Sci.* 2019;20:6249.
11. Zhang M, Wang S, Yi A, Qiao Y. microRNA-665 is down-regulated in gastric cancer and inhibits proliferation, invasion, and EMT by targeting PPP2R2A. *Cell Biochem Funct.* 2020;38:409-418.
12. Zhao J, Yang T, Ji J, Zhao F, Li C, Han X. RHPN1-AS1 promotes cell proliferation and migration via miR-665/Akt3 in ovarian cancer. *Cancer Gene Ther.* 2021;28:33-41.
13. Zhao XG, Hu JY, Tang J, Yi W, Zhang MY, Deng R, Mai SJ, Weng NQ, Wang RQ, Liu J, Zhang HZ, He JH, Wang HY. miR-665 expression predicts poor survival and promotes tumor metastasis by targeting NR4A3 in breast cancer. *Cell Death Dis.* 2019;10:479.
14. Wang W, Ying Y, Xie H, Li J, Ma X, He L, Xu M, Chen S, Shen H, Zheng X, Liu B, Wang X, Xie L. miR-665 inhibits epithelial-to-mesenchymal transition in bladder cancer via the SMAD3/SNAIL axis. *Cell Cycle.* 2021;20:1242-1252.
15. Chen J, Li X, Yang L, Li M, Zhang Y, Zhang J. CircASH2L promotes ovarian cancer tumorigenesis, angiogenesis, and lymphangiogenesis by regulating the miR-665/VEGFA axis as a competing endogenous RNA. *Front Cell Dev Biol.* 2020;8:595585.
16. Zhou P, Xiong T, Yao L, Yuan J. MicroRNA-665 promotes the proliferation of ovarian cancer cells by targeting SRCIN1. *Exp Ther Med.* 2020;19:1112-1120.
17. Ying X, Zhu J, Zhang Y. Circular RNA circ-TSPAN4 promotes lung adenocarcinoma metastasis by upregulating ZEB1 via sponging miR-665. *Mol Genet Genomic Med.* 2019;7:e991.
18. Huang C, Yue W, Li L, Li S, Gao C, Si L, Qi L, Cheng C, Lu M, Chen G, Cui J, Zhao R, Li Y, Tian H. Circular RNA hsa-circ-000881 suppresses the progression of lung adenocarcinoma *in vitro* via a miR-665/PRICKLE2 axis. *Ann Transl Med.* 2021;9:498.
19. Soady KJ, Tornillo G, Kendrick H, Meniel V, Olijnyk-Dallis D, Morris JS, Stein T, Gusterson BA, Isacke CM, Smalley MJ. The receptor protein tyrosine phosphatase PTPRB negatively regulates FGF2-dependent branching morphogenesis. *Development.* 2017;144:3777-3788.
20. Qi Y, Dai Y, Gui S. Protein tyrosine phosphatase PTPRB regulates Src phosphorylation and tumour progression in NSCLC. *Clin Exp Pharmacol Physiol.* 2016;43:1004-1012. Erratum in: *Clin Exp Pharmacol Physiol.* 2019;46:194.
21. Schmittgen TD, Livak KJ. Analyzing real-time PCR data by the comparative C_T method. *Nat Protoc.* 2008;3:1101-1108.
22. Li J, Sun D, Pu W, Wang J, Peng Y. Circular RNAs in cancer: biogenesis, function, and clinical significance. *Trends Cancer.* 2020;6:319-336.
23. Wang C, Tan S, Liu WR, Lei Q, Qiao W, Wu Y, Liu X, Cheng W, Wei YQ, Peng Y, Li W. RNA-Seq profiling of circular RNA in human lung adenocarcinoma and squamous cell carcinoma. *Mol Cancer.* 2019;18:134.
24. Verduci L, Strano S, Yarden Y, Blandino G. The circRNA-microRNA code: emerging implications for cancer diagnosis and treatment. *Mol Oncol.* 2019;13:669-680.
25. Huang ZY, Liao PJ, Liu YX, Zhong M, Sun AH, Jiang XC, Wang XP, Zhang M. Protein tyrosine phosphatase, receptor type B is a potential biomarker and facilitates cervical cancer metastasis via epithelial-mesenchymal transition. *Bioengineered.* 2021;12:5739-5748.
26. Hu Y, Yang C, Yang S, Cheng F, Rao J, Wang X. miR-665 promotes hepatocellular carcinoma cell migration, invasion, and proliferation by decreasing Hippo signaling through targeting PTPRB. *Cell Death Dis.* 2018;9:954.
27. Xia J, Li D, Zhu X, Xia W, Qi Z, Li G, Xu Q. Upregulated miR-665 expression independently predicts poor prognosis of lung cancer and facilitates tumor cell proliferation, migration and invasion. *Oncol Lett.* 2020;19:3578-3586.
28. Qi Y, Dai Y, Gui S. Corrigendum: Protein tyrosine phosphatase PTPRB regulates Src phosphorylation and tumour progression in NSCLC. *Clin Exp Pharmacol Physiol.* 2019;46:194. Erratum for: *Clin Exp Pharmacol Physiol.* 2016;43:1004-1012.